Biosensors and Bioelectronics 216 (2022) 114604

Contents lists available at ScienceDirect

Biosensors and Bioelectronics

journal homepage: www.elsevier.com/locate/bios

Accelerated antibiotic susceptibility testing of pseudomonas aeruginosa by monitoring extracellular electron transfer on a 3-D paper-based cell culture platform

Zahra Rafiee [a], Maryam Rezaie [a], Seokheun Choi [a,b,*]

[a] Bioelectronics & Microsystems Laboratory, Department of Electrical & Computer Engineering, State University of New York at Binghamton, Binghamton, NY, 13902, USA

[b] Center for Research in Advanced Sensing Technologies & Environmental Sustainability, State University of New York at Binghamton, Binghamton, NY, 13902, USA

ARTICLE INFO

Keywords:
Pseudomonas aeruginosa
Antimicrobial susceptibility testing
Extracellular electron transfer
Paper-based sensors
Electrical monitoring

ABSTRACT

Pseudomonas aeruginosa is the most important opportunistic pathogen leading to serious and life-threatening infections, especially in immunocompromised patients. Because of its remarkable capacity to resist antibiotics, the selection of the right antibiotics with the exact dose for the appropriate duration is critical to effectively treat the infections and prevent antibiotic resistance. Although conventional genotypic and phenotypic antibiotic susceptibility testing (AST) methods have been dramatically advanced, they have suffered from many technical and operational issues as a generalized antibiotic stewardship program. Furthermore, given that most microbial infections are caused by their biofilms, the existing AST methods do not provide evidence-based antibiotic prescribing guidance for biofilm-based infections because the results are based on individual bacteria traditionally grown in their planktonic form. In this work, we create an innovative susceptibility testing technique for *P. aeruginosa* that offers clinically relevant guidelines and widely adaptable stewardship to effectively treat the infections and minimize antibiotic resistance. Our approach evaluates the antibiotic efficacy by continuously monitoring the accumulated electrical outputs from the bacterial extracellular electron transfer (EET) process in the presence of antibiotics. Our innovative paper-based culturing 3-D scaffold promotes surface-associated growth of bacterial colonies and biofilms. The platform replicates a natural habitat for *P. aeruginosa* where it can grow similarly to sites it infects. Our technique enables an all-electrical, real-time, easy-to-use, portable AST that can be easily translatable to clinical settings. The entire procedure takes 96 min to provide evidence-based antimicrobial prescribing guidance for biofilm-based infections.

1. Introduction

Pseudomonas aeruginosa leads to substantial morbidity and mortality in immunocompromised or elder individuals, and the World Health Organization (WHO) and the U.S. Centers for Disease Control and Prevention (CDC) classify it as a critical opportunistic pathogen (Pang et al., 2019; Laborda et al., 2021). Because *P. aeruginosa* can survive many environments and their large genomes enable adaptation to adverse environmental conditions, *P. aeruginosa* evolves defense systems against various antibiotics through multi-faceted resistance mechanisms (Pang et al., 2019; Laborda et al., 2021). The rapid emergence and spread of antibiotic-resistant *P. aeruginosa* poses a great challenge for antibiotic therapy and clinical management of bacterial infections. Even worse, the misuse or overuse of the empiric broad-spectrum antibiotics accelerates the development of the multidrug-resistant *P. aeruginosa*, a so-called "superbug," causing an estimated 32,600 infections and 2700 deaths in the U.S. in 2017 (www.cdc.gov/DrugResistance/Biggest-Threat.html; Huang et al., 2020). Furthermore, weak regulations for antibiotic stewardship in many developing countries challenge the global efforts to mitigate the antibiotic resistance crisis, which is expected to be aggravated by emerging societal factors such as population aging, increased human migrations, and more infectious disease outbreaks induced by climate change (Dietvorst et al., 2020).

The discovery and development of antibiotics cannot be a permanent solution to effectively address antibiotic resistance because *P. aeruginosa* will likely resist the new antibiotics. Their inequitable worldwide

* Corresponding author. Bioelectronics & Microsystems Laboratory, Department of Electrical & Computer Engineering, State University of New York at Binghamton, Binghamton, NY, 13902, USA.
E-mail address: sechoi@binghamton.edu (S. Choi).

https://doi.org/10.1016/j.bios.2022.114604
Received 6 July 2022; Received in revised form 21 July 2022; Accepted 26 July 2022
Available online 6 August 2022

distribution can facilitate the emergence and dissemination of the drug-resistant pathogen (Dietvorst et al., 2020; Osaid et al., 2021). A better realistic and practical solution for the treatment of *P. aeruginosa* infections is for all health professionals worldwide to implement accurate, rapid, and accessible evidence-based treatment protocols in the beginning stage of bacterial infections. A worldwide acceptance of this accelerated antibiotic stewardship will eliminate many of the issues associated with drug-resistant bacteria. Providing rapid and inexpensive

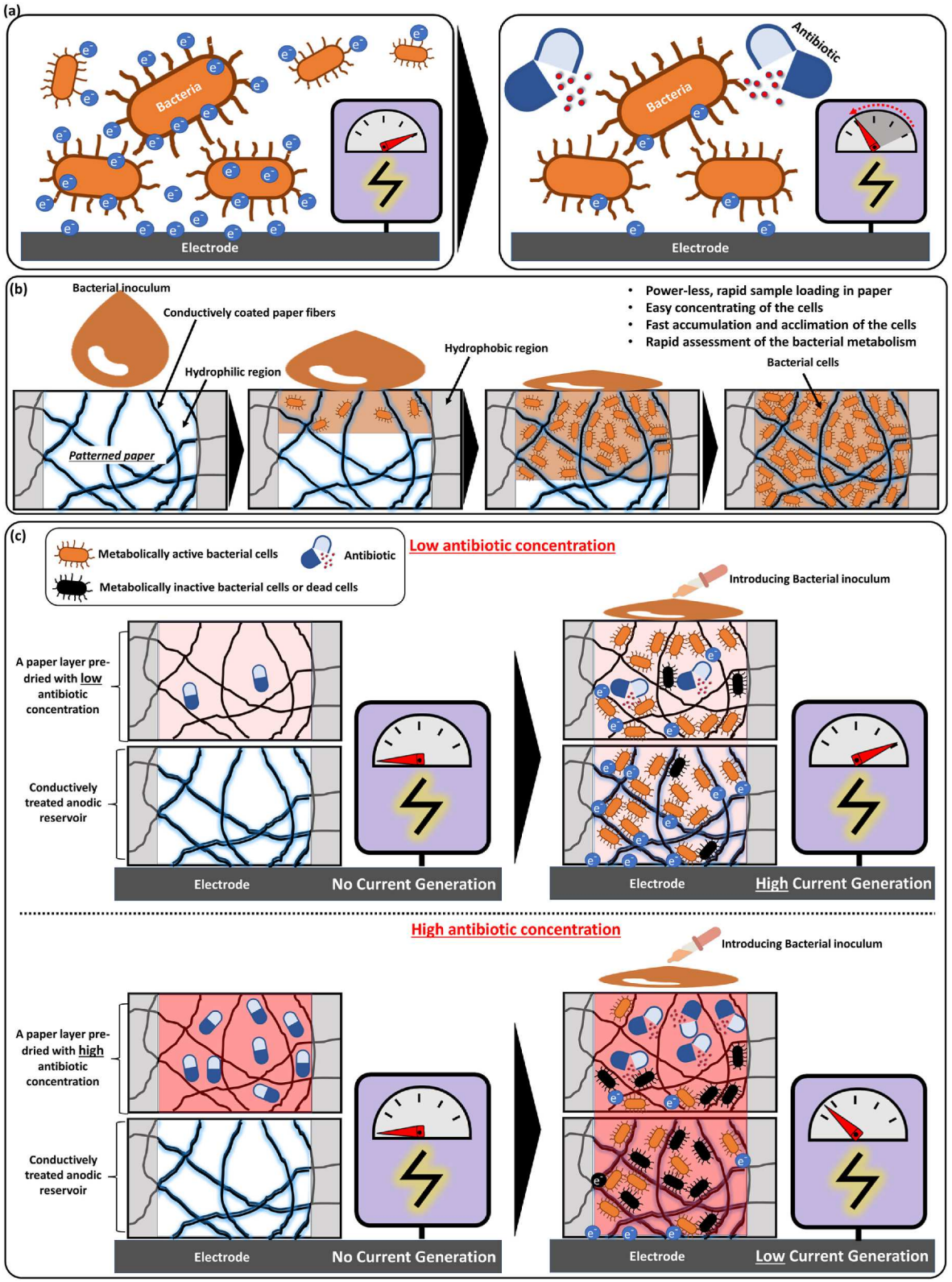

Fig. 1. Schematic illustration of our EET-based AST technique on paper culturing platfom. (a) Monitoring the accumulated electrical outputs from the bacterial EET process in the absence and presence of antibiotics. (b) Cultivating bacterial colonies and biofilms in the paper-based 3-D environment. (c) Our paper-based all-electrical EET-based AST technique with pre-loaded antibiotics.

decision-making information on antibiotic efficacy and promoting appropriate antibiotic use (i.e., selection of the right antibiotics with the exact dose for the appropriate duration) is critical to effectively treat infections and better control the spread of antibiotic resistance.

Although emerging genotypic antibiotic susceptibility testing (AST) methods rapidly provide information about many resistance genes for a species of bacteria, the technique has not been widely adopted because it needs bulky and expensive equipment, and well-trained personnel (Banerjee and Humphries, 2021). Moreover, the genotypic ASTs cannot provide quantifiable minimum inhibitory concentration (MIC) of antibiotics for effective infection treatment and are quite limited to prior knowledge of resistance genes (Mo et al., 2019). On the contrary, phenotypic ASTs have become the gold standard and a mechanism-independent universal method for surveillance of antibiotic resistance and diagnostics with the MIC value. The phenotypic ASTs (e.g., broth dilution) monitor bacterial growth in the presence of antibiotics, allowing exact phenotypic screening with direct clinical and therapeutic relevance (Behera et al., 2019; Leonard et al., 2018). However, the approaches require very time-consuming bacterial cultivation for initial growth and incubation to express the response to various antibiotic loads, leading to a turnaround time of at least 24 h. Moreover, the conventional phenotypic ASTs involve a relatively large amount of reagents and space, significantly increasing the total cost and the probability of human error (Shanmugakani et al., 2020). These limitations give medical doctors no choice but to select empirical antibiotic therapy in urgent situations, which makes the issue of antibiotic resistance worse (Dietvorst et al., 2020). Recently, the single-cell-based microfluidic AST technique promises to reduce the turnaround time, reagent amount, and space by confining the individual cells in a micro- or nano-sized environment (Campbell et al., 2016; Baltekin et al., 2017; Mohan et al., 2013); however, the technique requires complex device fabrication, sophisticated microfluidic flow control systems, expensive optical equipment, and tedious data management, which are not widely applicable in resource-limited settings. Furthermore, the microfluidic AST may not provide clinically relevant therapeutic guidance for bacterial infections because the results are based on individual homogenous cells grown in their planktonic form on a 2-D rigid culture platform. The 2-D environment is completely different from *in vivo* 3-D natural habitats when the cells respond to various chemical and physical cues (Yeon and Park, 2007; Mirbagheri et al., 2019). *P. aeruginosa* exists as clusters in 3-D and use quorum sensing inter-cellular communication to control virulence during infections (Thi et al., 2020; Tahernia et al., 2020a). In addition, their antibiotic resistance can be promoted by forming colonies which serve as a collective barrier to restrict antibiotic access to the cells (Pang et al., 2019).

This work creates an innovative susceptibility testing technique specific for *P. aeruginosa* that offers clinically relevant guidelines and widely adaptable stewardship to effectively treat the infections and reduce the spread of antibiotic resistance. Our approach evaluates the antibiotic efficacy by continuously monitoring the accumulated electrical outputs from the bacterial extracellular electron transfer (EET) in the presence of antibiotics (Fig. 1a). *P. aeruginosa* is a very well-known exoelectrogen that respires by releasing metabolically generated electrons extracellularly, which then can travel to an external electrode via self-produced redox-active mediators (Tahernia et al., 2020b; Ajunwa et al., 2022). The accumulated electrons directly reflect the bacterial viability and metabolism while the proliferating cell numbers are inversely proportional to antibiotic effectiveness. Usually, bacterial metabolism allows a rapid phenotypic evaluation of antibiotic susceptibility before the number of cells changes enough to allow traditional culture-based techniques to be successful (Xu et al., 2022; Swami et al., 2021).

In particular, the transferred electrons can be a faster and more sensitive and reliable transducing signal than the other cellular metabolites (e.g., dissolved O_2 (Liu et al., 2021), pyocyanin (Webster et al., 2015), etc.), and the monitoring of the electrons enables an all-electrical, real-time, easy-to-use, portable AST that can be easily translatable to clinical settings. Furthermore, our paper-based device platform provides a 3-D culture environment that can develop growth conditions similar to those of the infected sites by *P. aeruginosa* (Fig. 1b). The porous network of intertwined cellulose fibers works as a scaffold to mimic the bacterial 3-D natural habitats, providing an *in vivo* morphologic and physiologic environment better than the conventional 2-D platforms (e.g., Petri dishes, flasks, and glass slides) (Tahernia et al., 2020a). The intrinsic capillary force of paper promotes the immediate cell attachment and the formation of the bacterial colonies which are readily concentrated in a micro-liter paper reservoir without needing energy- and equipment-intensive external pumps or tubes (Fraiwan and Choi, 2014). The cellulose fibers are engineered with a poly(3,4-ethylened ioxythiophene):polystyrene sulfonate (PEDOT:PSS) polymer that conducts the electrons generated from *P. aeruginosa*. Therefore, rapid and sensitive assessment of the bacterial metabolic activities in the presence of antibiotics can be readily made from a low-volume sample and even a low concentration of the bacteria cells. The technique substantially reduces the time needed to form bacterial colonies and then incubate them with antibiotics.

A proof-of-concept demonstration of how meaningfully bacterial electrogenicity can be applied to the AST was introduced in our recent report (Gao et al., 2020). However, the need for the cumbersome long-term incubation time of planktonic bacteria in a separate tube with antibiotics could not translate the technology beyond laboratory novelty into practical, real-world monitoring of the antibiotic effectiveness against bacterial aggregates and biofilms. Moreover, the report failed to show how sensitively and rapidly the bacterial EET process can be used to monitor antibiotic efficacy. Also, an EET-based follow-up study by another group could not quantify the MIC values (Tibbits et al., 2022). Here, we demonstrate a practical and reliable approach to assess antibiotic effectiveness rapidly, sensitively, and continuously against *P. aeruginosa* by comprehensively exploring the bacterial electron transfer on a 3-D paper-based culturing platform. Six dried antibiotic concentrations are pre-loaded to simplify the testing workflow and reduce the incubation time (Fig. 1c). The paper origami techniques allow for simple device fabrication and operation while the paper-based 3-D and hydrophilic culturing environment allows rapid formation of bacterial colonies and effective distribution of antibiotics to individual cells. The validity, sensitivity, turnaround time, and reliability of this technique are discussed to show the practical efficacy of the bacterial electron transfer measurement on paper as a novel and effective AST approach for *P. aeruginosa.*

2. Results and discussion

2.1. Preparation and operation of the paper-based AST array

Bacterial EET is a promising field of study, named "electromicrobiology," that allows the development of innovative techniques for green energy production and energy-efficient wastewater treatment (Lovley, 2012). Moreover, the electrical outputs from the EET process can detect water toxicity because various toxic components can inhibit bacterial metabolic activity, slowing the transfer of electrons (Choi, 2022). Recently, our group successfully demonstrated that bacterial exoelectrogenic activities can access antibiotic effectiveness against *P. aeruginosa* by monitoring a distinct change in the electrical outputs from those antibiotics (Gao et al., 2020). The susceptibility of *P. aeruginosa* to antibiotics was continuously and sensitively evaluated by monitoring the electrical current harvested from bacterial metabolism in a microbial fuel cell (MFC).

However, much of this work is nascent; the evolution of the technology requires considerable exploration through comprehensive systematic integration and dramatic improvement in performance and operation. Furthermore, the technique does not provide antibiotic prescribing guidance for clinically relevant colony- or biofilm-based

infections because the results are from the measurement against planktonic cell growth. In this work, we use an array of 6 two-electrode MFCs integrated with a paper-based culturing platform as a rapid AST sensor to monitor the EET by *P. aeruginosa* grown in their colony and biofilm forms. By fabricating the device components on a single-sheet paper substrate and an origami-based folding of the 2-D sheet into a 3-D functional device, the MFC-based AST array was constructed, simplifying the fabrication, storage, and operation of the susceptibility testing (Fig. 2). The 2-D sheet paper included three functional tabs: (i) antibiotic-containing zones, (ii) conductively engineered anodic reservoirs, and (iii) wax-based ion exchange membranes and Ag_2O cathodic regions (Fig. 2a). All component boundaries were defined by well-controlled double-sided wax printing. The anodic reservoirs were prepared by tightly encapsulating the non-conductive cellulose fibers with a conductive PEDOT:PSS polymer, followed by hydrophilic treatment, so that the regions could be a conductive, porous, hydrophilic, and biocompatible environment for effectively inoculation of the exoelectrogenic *P. aeruginosa.* Each anodic reservoir had a 4 mm diameter that contained 5 μL. This 3-D environment efficiently harvests the electrons generated from the bacterial metabolism while ensuring a large area with favorable conditions for fast and dense bacterial adhesion and viability. An Ag_2O catalyst, which has been widely used for fuel cells (Xie et al., 2013), was incorporated for cathodic reactions. Graphite electrodes were screen-printed on the anodic and cathodic regions for electrical measurements. The anode and the cathode were electrochemically active and functioned as good support with respect to repeated potential cycling (Fig. S1). The CV area increased with the scanning speed, indicating a good rate capability. Dried 0, 2, 4, 8, 16, and 32 μg/mL concentrations of antibiotics were loaded into the antibiotic regions. The 3-D MFC-based AST array was directly constructed from the 2-D sheet of paper by folding along pre-defined creases and attaching the individual paper tabs with an adhesive spray (Fig. 2b). When the bacterial samples were introduced through the antibiotic regions, the cells were washed into the anodic reservoir along with the pre-loaded antibiotics (Fig. 1c). When the bacteria go through anaerobic cellular respiration to obtain biological energy, electron transfer from the cells to external electrode occurs. This bacterial EET unleashes a proton motive force for adenosine triphosphate (ATP) synthesis, the biological energy unit (Lovley, 2012). The antibiotic exposures inhibit bacterial metabolism and reduce electron and proton production. While the electrons are transferred to the anode, the protons diffuse across the wax-based ion exchange membrane and reduce Ag_2O to Ag at the cathode by combining with the electrons that traveled from the anode through an external circuit. To quantify the antibiotic effectiveness, we measured the accumulated output power through time with an external resistance of 47.5 kΩ. By taking a single additional step of the bacterial sample with a 6-channel pipette, we enabled multiplexed susceptibility testing of six antibiotic concentrations and pursued an all-electrical, real-time monitoring of the antibiotic efficacy, simplifying the AST protocol.

2.2. Cell seeding and colony cultivation in paper

More than 65% of microbial infections and more than 80% of chronic infections (e.g., urinary tract infections, cystic fibrosis lung infections, sinusitis, and osteomyelitis) are caused by microbial colonies and biofilms (Li et al., 2020; Sun et al., 2013). Usually, microbial colonies and biofilms are much more resistant to antibiotic treatment than planktonic

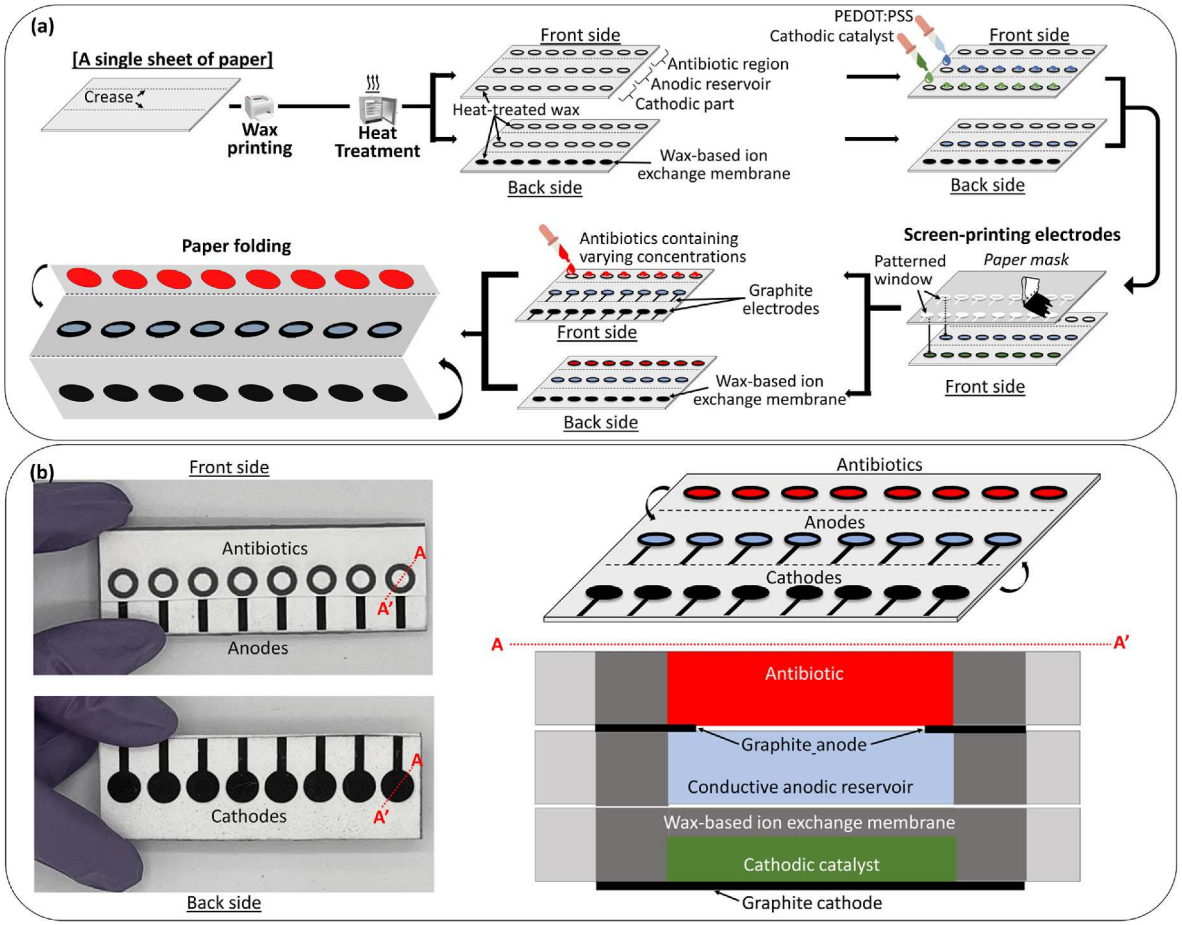

Fig. 2. Overview of the AST array fabrication. (a) Integration of the device components into a single paper sheet and origami-based folding of the 2-D sheet to form a 3-D device. (b) Pictures of the front and back fo the assembled device, and schematic diagam of the 2-D sheet and the cross-section of one unit in the array (A-A′).

cells. Nearly 80% of those infections cannot be treated with the MIC of antibiotics, which is normally effective against planktonic cells (Jamal et al., 2018). Because of the 3-D heterogeneous and long-term nature of bacterial colony formation, susceptibility testing for colonies remains challenging and there is no universally used standard colony and biofilm protocol for clinical use. While most natural biofilms grow on corrugated and porous 3-D media, none of the previous biofilm models cannot support the structurally complex 3-D environment (Jamal et al., 2018). Our paper-based culturing platform can innovatively serve as a 3-D scaffold for surface-associated growth of bacterial colonies and biofilms, allowing for effective mass transport of nutrients and gases through pores. Hydrophilic and biocompatible treated cellulose fibers rapidly accumulate and acclimate bacterial cells, reducing the time to detect a quantifiable electrical output even from the small concentration of the bacterial sample loaded. Furthermore, paper's intrinsic capillary ability to concentrate the bacterial cells in a microliter-sized reservoir can promote the easy and fast formation of a colony and biofilm. Scanning electron microscopy (SEM) images of *P. aeruginosa* of different concentrations demonstrate that the paper-based culture platform can readily and rapidly form densely packed bacterial colonies (Fig. 3). A bacterial sample with an optical density value at 600 nm (OD_{600}) of 2.5 was obtained after culture for 8 h and then diluted with sterile LB (Luria Broth) to acquire additional bacterial samples having 0.1, 0.5, and 1.0 OD_{600} (Fig. S2a). The concentration of 0.1 OD_{600} (~10^8 CFU/mL) corresponds to around 0.5 McFarland turbidity standard for conventional phenotypic ASTs. Even the lowest bacterial concentration, 0.1 OD_{600}, formed multiple aggregates over the paper substrate (Fig. 3a). The high porosity and the large pore size of the paper substrate compared to the size of the individual *P. aeruginosa* cells enabled sufficient nutrient exchange to support internal bacterial colony growth and form very thick multilayers (Fig. 3b, c, and 3d). Given that the development of mature biofilm is initiated by a very time-consuming reversible attachment of planktonic cells (Sun et al., 2013; Jamal et al., 2018), the strong capillary force of paper allows for rapid adsorption of the cells, readily and rapidly forming an aggregate at high cell density (Webster et al., 2015; Fraiwan and Choi, 2014). This high density of bacterial cells can facilitate bacterial communication through quorum sensing and expedite biofilm formation (Thi et al., 2020; Sun et al., 2013; Jamal et al., 2018).

2.3. Selection of the electrical quantity as a sensitive AST measurement

To effectively use the MFC as a sensor for AST, its electrical output as a measurement signal must be high and sensitive enough to distinguish bacterial metabolic changes with small antibiotic concentrations. Significant enhancement of the MFC electrical output was made by electrofluidic engineering of the anodic paper reservoir and cathodic overpotential reduction with the solid-state Ag_2O cathode on paper. Our up-to-date paper-based MFC technique was revolutionarily leveraged here as a sensitive AST platform (Gao and Choi, 2018; Landers and Choi, 2022). The water-dispersed conducting PEDOT:PSS polymer tightly coated the individual cellulose fibers, creating a conductive, biocompatible, porous, and hydrophilic scaffold for *P. aeruginosa* cells to have better adhesion and electrocatalytic activities. The Ag_2O cathode provides significant power from the low cathodic overpotential losses and fast reaction rate, and remains solid in water, leading to stable and reliable operation. Usually, basic electrical quantities including open-circuit voltages (OCVs), voltage outputs, currents, and powers, have been used as a potential sensing parameter reflecting bacterial metabolic activities (Cho et al., 2019). However, these parameters are very dependent on the bacterial sample concentration, requiring long cultivation and incubation times to observe meaningful data especially for low bacterial concentrations. As shown in Fig. S2, the electrical outputs rise considerably with bacterial concentration. The electrical outputs plateau when the bacterial concentration reaches 2.5 OD_{600}, and the 5.0 μL anodic reservoir is saturated with that concentration (Figs. S2b and S2c). We refer to that result as a saturated output. The concentration of 2.5 OD_{600} represents the maximum biofilm formation. (Fig. 3). However, as the concentration decreases, the electrical output becomes too small to sense. While quantifiable electrical outputs were generated from the bacterial concentration of 0.1 OD_{600} (Fig. S2b), the outputs were not strong enough to sensitively and continuously assess antibiotic effectiveness against bacterial metabolic changes (Fig. S3). The collectively harvested electrical outputs from a low-concentration group of cells become insufficient to measure reactions to an antibiotic. The limit of detection (LOD) is one of the most critical factors in effectively monitoring antibiotic efficacy because the standardized inoculum for the conventional AST goes down to a lower level of 0.1 OD_{600} which is equivalent to a 0.5 McFarland standard. In this work, we revolutionarily use "energy," by which we mean the accumulated power

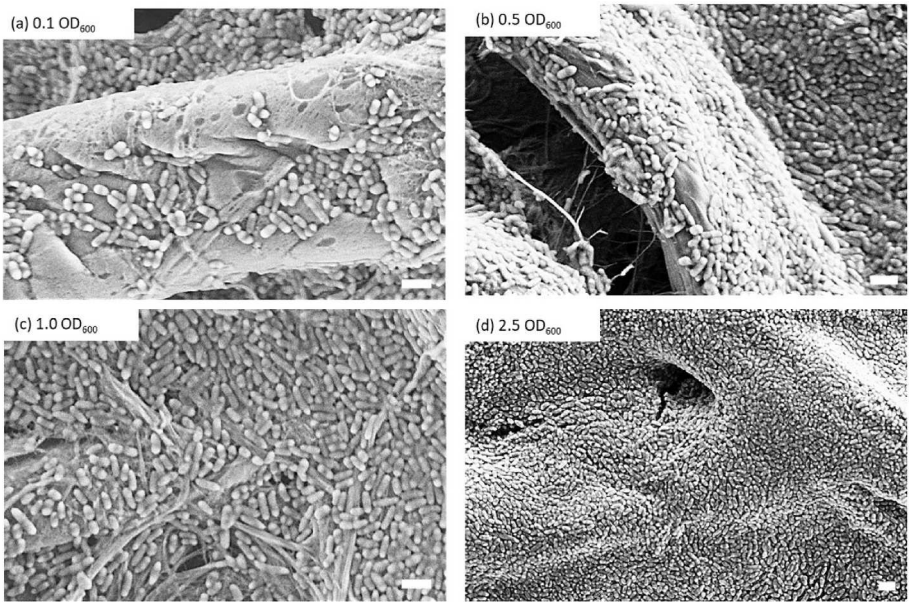

Fig. 3. SEM images of the paper reservoirs with different concentration of *P. aeruginosa*; (a) 0.1, (b) 0.5, (c) 1.0, and (d) 2.5 of the optical density (OD) at 600 nm (OD_{600}) (scale bar: 2 μm).

outputs through time as the measurement signal. The energy "E" was calculated as described in the following,

$$E = \sum_{0}^{T} P \cdot \Delta t$$

where T is total accumulation time in seconds, P is the measured output power at time t.

The accumulations become sufficient to show small variations in antibiotic effectiveness even with MFCs having low bacteria concentrations. For the experiment, we selected the external resistance of 47.5 kΩ to be connected between the anode and the cathode of the MFC, generating the maximum power. The resistor extracts the maximum power output from the MFC (Figs. S2b and S3). When the antibiotic exposure sufficiently inhibits the metabolism and growth of the bacteria, the energy will plateau.

2.4. All-electrical monitoring of antibiotic susceptibility

P. aeruginosa is a weak exoelectrogen that relies on self-produced redox-active mediators for their EET (Ajunwa et al., 2022). To assess the effects of the antibiotics by measuring energy, we must eliminate contributors to electrical variations before the AST. To do that, we remove all redox-active mediators produced during the initial cultivation and resuspend the bacterial samples in a new medium. Moreover, our EET-based AST on the paper platform requires an accumulation period to allow the bacterial cells to move along the antibiotics to the anodic area, adhere physically to the treated cellulose fibers, and start to generate the redox-active mediators responsive to the antibiotics. Because *P. aeruginosa* can grow with an average doubling time of about 30 min in a rich LB medium even though the paper substrate rapidly absorbs the bacterial sample and immediately promotes the cell attachment, we waited at least 30 min before starting the AST procedure.

Usually, the maximum electrical outputs are extracted from exoelectrogens in anoxic or anaerobic conditions because oxygen is the most preferred natural electron acceptor because of its high standard potential (Tahernia et al., 2020b; Lovley, 2012). Oxygen can divert metabolically produced electrons from the external electrode, leading to a significant reduction in electrical output (Choi et al., 2011). Also, oxygen shows toxic effects on some exoelectrogens such as *Geobacter* species (Yang et al., 2019). However, oxygen reveals a positive effect on the growth and the EET of aerobic or facultative exoelectrogens such as *P. aeruginosa* (Yang et al., 2019). Furthermore, our paper-based culturing platform promoted internal bacterial attachment filling the pores within the cellulose fibers (Fig. 3), mitigating the oxygen invasion, and the treatment of the biocompatible PEDOT:PSS polymer significantly improved the EET rate even in the aerobic condition by indirectly mediating the process (Tahernia et al., 2020b). As shown in Fig. S2d, our MFC-based AST sensor with *P. aeruginosa* (2.5 OD_{600}) showed an electricity loss of only less than 15% under aeration, demonstrating its practical efficacy in an actual natural environment.

Fig. 4 shows the energy outputs measured from our AST sensor for the different bacterial and antibiotic concentrations. The outputs, which were calculated by subtracting the aseptic control (only LB without bacteria) with the antibiotic from the bacterial sample with the antibiotic, represent the direct antibiotic effectiveness against the specific concentrations of *P. aeruginosa.* Those reference-compensated values eliminate all surrounding interferences and abiotic background noises. Overall, the initial inoculum cell concentration considerably affects the susceptibility of bacteria to antibiotics (Fig. 4). If energy plot plateaus, then the bacterial sample is susceptible to the antibiotic as the steady output indicates bacterial population growth has stopped. For the lowest concentration with 0.1 OD_{600}, their metabolic activities were inhibited even with the lowest antibiotic concentration of 2 μg/mL, thus generating a flat energy plot (Fig. 4a). The gold standard broth microdilution (BMD) that uses a much smaller bacterial concentration (~0.001 OD_{600}) shows "resistant" with 2 μg/mL gentamicin (Table 1). However, we believe our paper-based culturing platform shows a much more reliable result because it replicates the natural, 3-D habitat of the bacteria. The

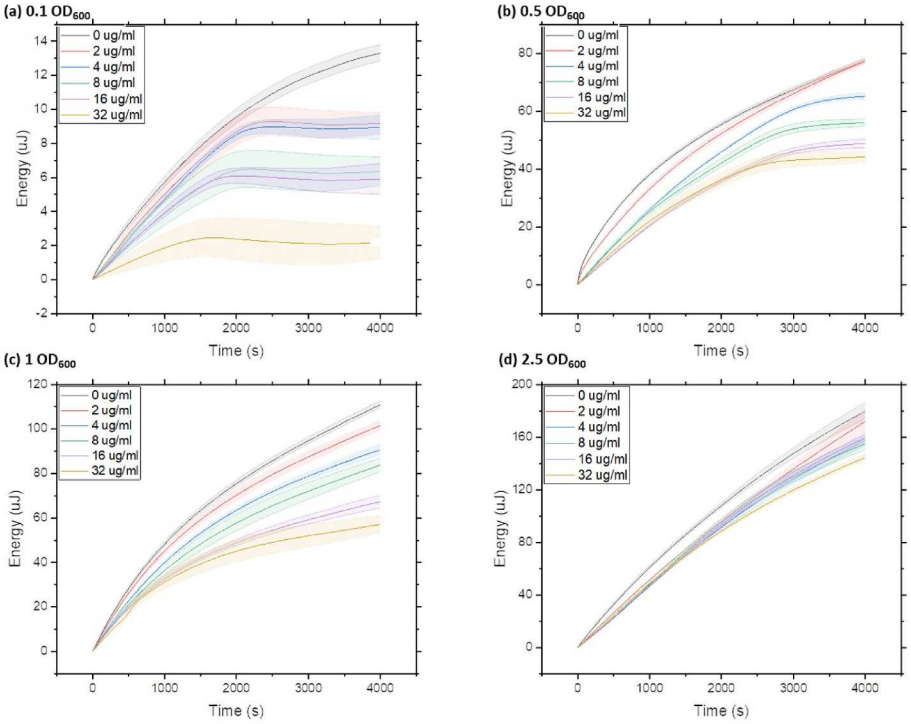

Fig. 4. Electrical energy generated from the MFC-based AST array with respect to inoculum and antibiotic concentrations. The energy is measured in micro-jules with varying bacterial concentrations of (a) 0.1 OD_{600}, (b) 0.5 OD_{600}, (3) 1.0 OD_{600}, and (4) 2.5 OD_{600}. All experimental data shown in this work were performed by repeating identical assays at least three times. The shaded area shows standard errors of those experimental replicates.

Table 1
Summary of the gold standard BMD and our AST results with different antibiotic concentrations.

	AST	Antibiotic concentration					
		0 μg/ml	2 μg/ml	4 μg/ml	8 μg/ml	16 μg/ml	32 μg/ml
Standard BMD	Susceptible (S)/ Resistant (R)	R	R	S	S	S	S
Our MFC-based AST array	S/R - 0.1 OD_{600}	R	S	S	S	S	S
	S/R - 0.5 OD_{600}	R	R	S	S	S	S
	S/R - 1.0 OD_{600}	R	R	R	R	R	R
	S/R - 2.5 OD_{600}	R	R	R	R	R	R

platform delivers the antibiotic more effectively to more individual cells than happens in the broth.

The 0.5 OD_{600} sample of a biofilm form shows "susceptible" with the concentration of 4 μg/mL gentamicin and more, which is in good agreement with the BMD method in their planktonic form (Fig. 4b and Table 1). Generally, as the antibiotic concentration decreased, the plateau of the energy output, if any, was delayed (Fig. 4a and b). The plateau starting point shows the time to the onset of the termination of bacterial metabolic activity and growth if the antibiotic is effective. The 0.1 OD_{600} sample has the onset points at around 1500, 1800, 2000, 2200, and 2300 s with 32 μg/mL, 16 μg/mL, 8 μg/mL, 4 μg/mL, and 2 μg/mL antibiotic concentration, respectively, while the 0.5 OD_{600} counterpart has much delayed points at 2700, 3000, 3200, and 3400 s with 32 μg/mL, 16 μg/mL, 8 μg/mL, and 4 μg/mL antibiotic concentration, respectively (No saturation with 2 μg/mL) (Fig. 4a and b). That indicates the decreased antibiotic efficacy on bacteria in colonies and biofilms with increasing bacterial numbers. Higher cell densities display measurable metabolic activity and growth even with very inhibitory concentrations of the antibiotic while lower cell densities show metabolic inhibition even in the presence of a reportedly resistant concentration of the antibiotic. In that sense, Table 1 is important to access the antibiotic effectiveness against biofilms with different cell densities.

The slope of the energy curve determines the bacterial metabolic speed. The antibiotic inhibits the bacterial metabolism, decreasing the slope, while higher cell densities show the increasing slope, which reveals greater resistance to the antibiotic. Notably, continuous inhibition does not necessarily express resistance. For example, 1.0 and 2.5 OD_{600} samples show a dramatic reduction in the slope with the increasing antibiotic concentration, but no plateaus are observed, indicating that none of the antibiotic concentrations can effectively deactivate the metabolism and growth of *P. aeruginosa* grown in their biofilm form.

To further characterize bacterial inhibition, all the energy outputs were normalized to each bacterial sample without antibiotics at 3000 s and 4000 s of the AST inoculation time (Fig. 5 and Fig. S4). The normalized results well demonstrate how much bacterial metabolic activities and their EETs decrease with different antibiotic concentrations according to the cell density in the biofilm form. Our AST technique is sensitive enough to display even minute differences in the normalized energy output caused by changes in antibiotic effectiveness. The inoculation times of 3000 s and 4000 s were sufficient to reflect the bacterial metabolic activities under different antibiotic concentrations. As the bacteria become more resistant to the antibiotic, their collective metabolism increases and the energy produced becomes very close to the sample without an antibiotic. This result indicates that antibiotic guidelines must be provided according to the actual bacterial concentration on the infected sites. Our paper-based culturing platform can readily and controllably replicate the bacterial colonies and biofilms with different inoculum concentrations. Furthermore, the MFC-based AST technique can continuously and rapidly monitor the bacterial responses to the antibiotic in real-time.

2.5. Validation, turnaround time, and reliability

This work is part of a global effort to enable an innovative, rapid, and easy-to-use, AST platform for pathogenic biofilms and thus provide effective antibiotic treatment guidelines while minimizing the unnecessary use of antibiotics. Genotypic and phenotypic AST methods have dramatically advanced to determine the antibiotic susceptibility of planktonic bacterial cells. However, biofilm antibiotic susceptibility depends on laborious and time-consuming procedures including colony and biofilm formation. Typically, the formed biofilms are exposed to antibiotics, and then bacteria are dislodged for microscopic examination of viability. The available standard biofilm protocol and susceptibility testing is very limited and the results do not seem clinically relevant. The proposed work of this study is unique. No other group has proposed an AST platform for colonies and biofilms that can provide real-time all-electrical monitoring capability with rapid microbial aggregate formation. Depending on the initial cell density, the MIC values generated from our colony- and biofilm-based AST technique are more or less related to the ones obtained from the standard planktonic-based BMD method validating our technique for *P. aeruginosa* biofilm. In particular, our 3-D paper culturing platform showed a better testing environment for antibiotic effectiveness against bacterial aggregates. We expect that a real clinical situation with biofilm-associated infections can be more reliably diagnosed and effectively cured by using our innovative testing and culturing platform.

The phenotypic ASTs generally require a relatively long time to form thick biofilms *in vitro* and monitor the effectiveness of an antibiotic. Our MFC-based AST technique on a 3-D paper culturing platform can provide a rapid electrical assessment, allowing early diagnostic analysis of antibiotic resistance to a 3-D biofilm which is rapidly and controllably formed within the engineered cellulose fibers. While initial enrichment

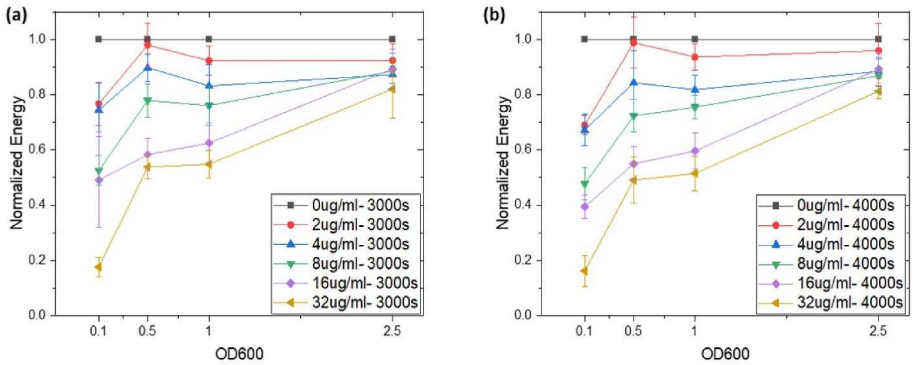

Fig. 5. Normalized energy outputs (as a function of inoculum concentrations) generated from samples with varying antibiotic concentrations. The energy is measured at (a) 3000 s and (b) 4000 s of inoculation time.

from a clinical sample is commonly required for all phenotypic ASTs, our technique significantly reduces start-up time for bacterial accumulation, biofilm formation, and inoculation time with antibiotics for the AST. Even with the 30 min waiting time before the AST, the procedure takes only 96 min to provide evidence-based antimicrobial prescribing guidance for biofilm-based infections.

2.6. Future work

Normally, pathogenic *P. aeruginosa* does not exist as single species. Rather, they exist as part of complex polymicrobial biofilm communities (Thi et al., 2020). Each strain exists for a specific purpose. One example includes syntrophic relationships where organisms can participate in cross-feeding. Various microorganisms have been shown to produce substances that are consumed by other species in the community. These polymicrobial biofilms are extremely difficult to model for an antibiotic effectiveness test. We believe that a 3-D multi-laminate paper stack can provide a new strategy for rapid layer-by-layer polymicrobial biofilm formation. Our MFC-based paper AST platform will generate many different experimental setups to better understand key mechanisms underlying antibiotic efficacy throughout the biofilm and other fundamental factors determining antibiotic effectiveness.

While this work is limited to exoelectrogenic *P. aeruginosa*, our MFC-based AST can work even for non-exoelectrogenic pathogens by adding redox mediators to enable the electron transfer. Previously, the mediated MFCs or the bacterial electrochemical cells were successfully demonstrated as a sensor for environmental toxicity testing (Gonzalez-Pabon et al., 2021; Chung and Dhar, 2021; Vigues et al., 2018). We expect various pathogens to be explored by our AST technique.

3. Conclusion

In this work, we provided a powerful yet simple method to assess antibiotic effectiveness against engineered biofilm models formed from a low volume sample (~10 μL), which enables rapid (<2 h), and real-time monitoring. The proposed AST approach continuously monitored EET by bacterial cells in biofilms, parallelly and controllably formed on a paper-based sensing array. The number of transferred electrons reflected the bacterial metabolic activities and their growth while the metabolically active cell numbers are inversely proportional to antibiotic effectiveness. The electrons collectively harvested from the group of cells in a biofilm were strong enough as a transducing signal to monitor bacterial growth and antibiotic susceptibility sensitively and continuously, and the 3-D paper culturing substrate provided a new strategy to replicate natural bacterial habitats and form biofilm in a controllable and rapid manner. The anodic paper reservoirs treated with a PEDOT:PSS polymer provided a porous, conductive, and biocompatible environment for effective inoculation of bacterial cells while the solid-state Ag_2O cathode offered simple device structure and improved function without exposing the cathode to the air. This work successfully created an all-electrical real-time monitoring approach for antibiotic susceptibility by measuring bacterial EET and established a biofilm model. This work will provide valuable information on the antibiotic efficacy and the right doses for treatment against biofilm-related infections.

4. Materials and methods

Fabrication of the paper-based AST array The MFC-based AST array was constructed by folding a 2-D sheet of paper (Whatman 3 MM CHR filter paper) integrating a pre-loaded antibiotic region and MFC components (i.e., anodic reservoirs, wax-based ion exchange membranes, and cathodes) (Fig. 2 and Fig. S5). The 2-D paper was designed to have three folding tabs that monolithically incorporated individual device components. The components were well defined by hydrophobic wax boundaries printed from a Xerox Phasor printer (ColorQube 8570), followed by heat treatment (at 160 °C for 50 s) to melt the wax throughout the paper. The anodic reservoirs were conductively engineered by introducing the mixture of PEDOT:PSS (Clevios PH1000, Heraeus) and dimethyl sulfoxide (DMSO, Sigma Aldrich). Additional treatment with 3-glycidoxypropy-trimethoxysilane was necessary to increase the hydrophilicity of the anodic reservoirs. The wax penetration was well controlled to form a relatively thin wax-based ion exchange membrane so that the metabolically produced protons can be diffused to the cathode while the electrons move externally along the circuit. The cathodic compartments were prepared by introducing an Ag_2O catalyst diluted in the PEDOT:PSS solution. The solid-state Ag_2O cathodes typically produce higher performance than Pt-based air-cathodes because of their very low cathodic over-potential (Landers and Choi, 2022). Finally, the graphite ink (E3449, Ercon) was screen-printed on the anodic and cathodic regions as electron collectors. More details on the chemical composition and concentration were well discussed in our previous reports (Yang and Choi, 2018; Landers and Choi, 2022).

Bacterial inoculum and antibiotics *P. aeruginosa* PAO1 was grown in LB (pH 7.0) consisting of 10 g/L tryptone, 5 g/L NaCl, and 5 g/L yeast and cultivated aerobically for about 8 h at 37 °C to an OD_{600} of 2.5, corresponding to around 10^9 cells/mL. The culture was then centrifuged at 4000 rpm for 4 min. After the supernatant was discarded, the cell pellet was resuspended in fresh LB medium by agitation with a vortexer. Then, the culture was subsequently diluted to prepare starting concentrations of 0.1, 0.5, 1.0, and 2.5 OD_{600}. One of the aminoglycosides, gentamicin, which is commonly used to treat *P. aeruginosa* infections, was selected as a model antibiotic. Gentamicin can interfere with protein synthesis and disrupt the outer membrane of *P. aeruginosa* (Martin and Beveridge, 1986). To acquire the MIC values according to different bacterial concentrations, the gentamicin was prepared in six dilutions (0, 2, 4, 8, 16, & 32 μg/ml in sterile LB) and pre-loaded on the paper-based AST array, followed by air-drying to enable fast and simple testing with a single bacterial sample loading step.

Bacterial fixation and SEM imaging The fixation of the bacterial cell on the cellulose fibers was carried out by using 2.5% glutaraldehyde in 0.1 M phosphate buffer saline for 10 h. Then the samples were dehydrated in ascending ethanol series (35%, 50%, 75%, 95%, and 100%). Following dehydration, the samples were dried overnight in a desiccator. The samples were coated with a thin film of carbon (208HR Turbo Sputter Coater, Cressington Scientific Instruments, UK) and examined by a field emission scanning electron microscopy (FE-SEM, Supra 55 VP, Carl Zeiss AG, German).

Electrical measurement setup The power outputs and polarization curves were first acquired from the MFCs by measuring the voltage values at various external resistors (No resistor, 470 kΩ, 250 kΩ, 162 kΩ, 100 kΩ, 71 kΩ, 47.5 kΩ, 32 kΩ, 22 kΩ, 15 kΩ, 10 kΩ, 2kΩ, 1.5 kΩ, 0.45 kΩ, and 0.35 kΩ), and calculating the corresponded electrical quantities. Power and current densities were normalized to the anode surface area. All the maximum power outputs were obtained at 47.5 kΩ where the external resistance is equal to the internal resistance of the MFC. The continuous monitoring of the electrical outputs against antibiotics was performed with a data acquisition system (DI-4108U, DataQ, USA) through the external resistor of 47.5 kΩ.

AST procedures 10 μL of each bacterial sample of 0.1, 0.5, 1.0, and 2.5 OD_{600} was dropped on each AST array containing gentamicin in different concentrations. Each antibiotic well and anodic reservoir on paper can accommodate about 5 μL of sample volume, respectively. The paper-based device platform wicked the bacterial sample through capillary action while the sample moved along with the pre-loaded antibiotic to the anodic reservoir. Before the antibiotic efficacy was electrically monitored, we waited 30 min to provide enough time for bacterial accumulation and acclimation so that they are ready to produce the redox-active compounds for bacterial EET. The accumulated power over time was continuously monitored while bacterial metabolic activities are inhibited with the antibiotics, decreasing their electron transfer reactions.

Broth microdilution (BMD) The MIC values determined by our technique with bacterial colonies and biofilms were compared to the gold standard broth microdilution (BMD) which is widely used for the planktonic form of bacteria. The BMD protocol followed the Clinical and Laboratory Standards Institute (CLSI) guidelines (Wiegand et al., 2008).

Statistical analysis All experimental data shown in this work were performed by repeating identical assays at least three times. Data were represented as the mean ± standard errors of those experimental replicates.

CRediT authorship contribution statement

Zahra Rafiee: Investigation, Methodology, Formal analysis, Data curation, Validation, Software. **Maryam Rezaie:** Investigation, Formal analysis. **Seokheun Choi:** Conceptualization, Supervision, Project administration, Funding acquisition, Writing – original draft, Writing – review & editing, finalization.

Declaration of competing interest

The authors declare that they have no known competing financial interests or personal relationships that could have appeared to influence the work reported in this paper.

Data availability

Data will be made available on request.

Acknowledgments

This work was supported mainly by the National Science Foundation (CBET #2100757) and partially by the National Science Foundation (ECCS #2020486, and ECCS #1920979).

Appendix A. Supplementary data

Supplementary data to this article can be found online at https://doi.org/10.1016/j.bios.2022.114604.

References

Ajunwa, O.M., Odeniyi, O.A., Garuba, E.O., Nair, M., Marsili, E., Onilude, A.A., 2022. World J. Microbiol. Biotechnol. 38, 90.
Baltekin, O., Boucharin, A., Tano, E., Andersson, D.I., Elf, J., 2017. Proc. Natl. Acad. Sci. USA 114, 9170–9175.
Banerjee, R., Humphries, R., 2021. Front. Med. 8, 635831.
Behera, B., Vishnu, A., Chatterjee, S., Sitaramgupta, V.S.N., Sreekumar, N., Nagabhushan, A., Rajendran, N., Prathik, B.H., Panday, H.J., 2019. Biosens. Bioelectron. 142, 111552.
Campbell, J., McBeth, C., Kalashnikov, M., Boardman, A.K., Sharon, A., Sauer-Budge, A. F., 2016. Biomed. Microdevices 18, 103.
Cho, J., Gao, Y., Choi, S., 2019. Sensors 19, 5452.
Choi, S., 2022. Small 18, 2107902.
Choi, S., Lee, H.-S., Yang, Y., Parameswaran, P., Torres, C.I., Rittmann, B.E., Chae, J., 2011. Lab Chip 11, 1110–1117.
Chung, T.H., Dhar, B.R., 2021. Biosens. Bioelectron. 192, 113485.
Dietvorst, J., Vilaplana, L., Uria, N., Macro, M., Munoz-Berbel, X., 2020. Trends Anal. Chem. 127, 115891.
Fraiwan, A., Choi, S., 2014. Phys. Chem. Chem. Phys. 16, 26288–26293.
Gao, Y., Choi, S., 2018. Advanced Materials Technologies 3, 1800118.
Gao, Y., Ryu, J., Liu, L., Choi, S., 2020. Biosens. Bioelectron. 168, 112518.
Gonzalez-Pabon, M.J., Corton, E., Figueredo, F., 2021. Chemosphere 265, 129101.
Huang, W., Hamouche, J.E., Wang, G., Smith, M., Yin, C., Dhand, A., Dimitrova, N., Fallon, J.T., 2020. Int. J. Mol. Sci. 21, 1026.
Jamal, M., Ahmad, W., Andleeb, S., Jalil, F., Imran, M., Nawaz, M.A., Hussain, T., Ali, M., Rafiq, M., Kamil, M.A., 2018. J. Chin. Med. Assoc. 81, 7–11.
Laborda, P., Sanz-Garcia, F., Hernando-Amado, S., Martinez, J.L., 2021. Curr. Opin. Microbiol. 64, 125–132.
Landers, M., Choi, S., 2022. Nano Energy 97, 107227.
Leonard, H., Colodner, R., Halachmi, S., Segal, E., 2018. ACS Sens. 3, 2202–2217.
Li, Y., Xiao, P., Wang, Y., Hao, Y., 2020. ACS Omega 5, 22684–22690.
Liu, Y., Lehnert, T., Magr, T., Gijs, M.A.Ml, 2021. Lab Chip 21, 3520–3531.
Lovley, D.R., 2012. Annu. Rev. Microbiol. 66, 391–409.
Martin, M.L., Beveridge, T.J., 1986. Antimicrob. Agents Chemother. 29, 1079–1087.
Mirbagheri, M., Adibnia, V., Hughes, B.R., Waldman, S.D., Banquy, X., Hwang, D.K., 2019. Mater. Horiz. 6, 45–71.
Mo, M., Yang, Y., Zhang, F., Jing, W., Iriya, R., Popovich, J., Wang, S., Grys, T., Haydel, S.E., Tao, N., 2019. Anal. Chem. 91, 10164–10171.
Mohan, R., Mukherjee, A., Sevgen, S.E., Sanpitakseree, C., Lee, J., Schroeder, C.M., Kenis, P.J.A., 2013. Biosens. Bioelectron. 49, 118–125.
Osaid, M., Chen, Y., Wang, C., Sinha, A., Lee, W., Gopinathan, P., Wu, H., Lee, G., 2021. Lab Chip 21, 2223–2231.
Pang, Z., Raudonis, R., Glick, B.R., Lin, T., Cheng, Z., 2019. Biotechnol. Adv. 37, 177–192.
Shanmugakani, R.K., Srinivasan, B., Glesby, M.J., Westblade, L.F., Cardenas, W.B., Raj, T., Erickson, D., Mehta, S., 2020. Lab Chip 20, 2607–2625.
Sun, F., Qu, F., Ling, Y., Mao, P., Xia, P., Chen, H., Zhou, D., 2013. Future Microbiol. 8, 877–886.
Swami, P., Sharma, A., Anand, S., Gupta, S., 2021. Biosens. Bioelectron. 182, 113190.
Tahernia, M., Mohammadifar, M., Choi, S., 2020a. Micromachines 11, 99.
Tahernia, M., Mohammadifar, M., Gao, Y., Panmanee, W., Hassett, D.J., Choi, S., 2020b. Biosens. Bioelectron. 162, 112259.
Thi, M.T.T., Wibowo, D., Rehm, B.H.A., 2020. Int. J. Mol. Sci. 21, 8671.
Tibbits, G., Mohamed, A., Call, D.R., Beyenal, H., 2022. Biosens. Bioelectron. 197, 113754.
Vigues, N., Pujol-Vila, F., Marquez-Maqueda, A., Munoz-Berbel, X., Mas, J., 2018. Anal. Chim. Acta 1036, 115.
Webster, T.A., Sismaet, H.J., Chan, I.J., Goluch, E.D., 2015. Analyst 140, 7195–7201.
Wiegand, I., Hilpert, K., Hancock, R.E.W., 2008. Nat. Protoc. 3, 163–175.
Xie, X., Ye, M., Hsu, P., Liu, N., Criddle, C.S., Cui, Y., 2013. Proc. Natl. Acad. Sci. USA 110, 15925–15930.
Xu, X., Chen, S., Yu, Y., Virtanen, P., Wu, J., Hu, Q., Koskiniemi, S., Zhang, Z., 2022. Sens. Actuators: B. Chem. 357, 131458.
Yang, J., Cheng, S., Li, P., Huang, H., Cen, K., 2019. iScience 13, 163–172.
Yeon, J.H., Park, J., 2007. Biochip J. 1, 17–27.